EUROPEAN COMMISSION
European Research Area

CArbon-14 Source Term

CAST

Final report on ^{14}C release and speciation from Zircaloy (D3.15)

Author(s):

Michel HERM[1], Tomofumi SAKURAGI[2], Ernesto GONZÁLEZ-ROBLES[1], Melanie BÖTTLE[1], Nikolaus MÜLLER[1], Elke BOHNERT[1], Ron DAGAN[3], Stefano CARUSO[4] Bernhard KIENZLER[1], Volker METZ[1]

[1] Karlsruhe Institute of Technology, Institute for Nuclear Waste Disposal, Karlsruhe, Germany
[2] Radioactive Waste Management Funding and Research Center, Tokyo, Japan
[3] Karlsruhe Institute of Technology, Institute for Neutron Physics and Reactor Technology, Karlsruhe, Germany
[4] Radioactive Materials Division, National Cooperative for the Disposal of Radioactive Waste, Wettingen, Switzerland

Date of issue of this report: 09/11/2017

The project has received funding from the European Union's Seventh Framework Programme for research, technological development and demonstration under grant agreement no. 604779, the CAST project'		
Dissemination Level		
PU	Public	**X**
RE	Restricted to the partners of the CAST project	
CO	Confidential, only for specific distribution list defined on this document	

CAST – Project Overview

The CAST project (CArbon-14 Source Term) aims to develop understanding of the potential release mechanisms of carbon-14 from radioactive waste materials under conditions relevant to waste packaging and disposal to underground geological disposal facilities. The project focuses on the release of carbon-14 as dissolved and gaseous species from irradiated metals (steels, Zircaloys), irradiated graphite and from ion-exchange materials as dissolved and gaseous species.

The CAST consortium brings together 33 partners with a range of skills and competencies in the management of radioactive wastes containing carbon-14, geological disposal research, safety case development and experimental work on gas generation. The consortium consists of national waste management organisations, research institutes, universities and commercial organisations.

The objectives of the CAST project are to gain new scientific understanding of the rate of re-lease of carbon-14 from the corrosion of irradiated steels and Zircaloys and from the leaching of ion-exchange resins and irradiated graphites under geological disposal conditions, its speciation and how these relate to carbon-14 inventory and aqueous conditions. These results will be evaluated in the context of national safety assessments and disseminated to interested stakeholders. The new understanding should be of relevance to national safety assessment stakeholders and will also provide an opportunity for training for early career researchers.

For more information, please visit the CAST website at:
http://www.projectcast.eu

CAST		
Work Package: 3	CAST Document no. :	Document type:
Task: 3.3	CAST-2017-D3.15	R = report
Issued by: KIT		Document status:
Internal no. : Reference to author's internal document number		Draft

Document title
Final report on ^{14}C release and speciation from Zircaloy (D3.15)

Executive Summary

In this report the work performed by the Radioactive Waste Management Funding and Research Center (RWMC) and the Karlsruhe Institute of Technology (KIT) with support from the National Cooperative for Disposal of Radioactive Waste (NAGRA, Switzerland) within work package 3 of the CAST project is summarized.

In the following sections, the thermodynamic modelling of ^{14}C in Zircaloy is presented as well as the experimentally determined radionuclide inventory in the irradiated cladding and the chemical form of ^{14}C released from the Zircaloy.

Furthermore, corrosion rates of unirradiated and irradiated Zircaloy as well as the instant release fraction (IRF) are discussed in this report.

KIT performed digestion experiments under acidic/anoxic conditions using irradiated Zircaloy-4. The inventory of ^{14}C was experimentally determined to $3.7(\pm0.4)\times10^4$ Bg/g and is in good agreement with activation calculations. About (88 ± 10)% of the ^{14}C inventory present in the studied Zircaloy-4 is released as gaseous organic ^{14}C-bearing compounds into the gas phase during acid digestion. On the contrary, about (11 ± 10)% remains as dissolved organic ^{14}C-bearing compounds in the acidic digestion liquor. A very low content of inorganic ^{14}C-bearing compounds (< 1%) is found in all experiments, both in the gaseous and aqueous phases.

RWMC have performed the corrosion experiment using nonirradiated and irradiated Zircaloy for long-term. The corrosion rates for nonirradiated Zircaloy decreased with time and increased as the temperature increased, but the influence of pH and other chemical components of the solution on the rate was not significant. The equivalent corrosion rate of irradiated Zircaloy-2 obtained from leached 14C assuming congruence with corrosion was less than that of unirradiated Zircaloy. Since this cannot be sufficiently explained with only the difference of the test condition (temperature), the congruence of 14C leaching with corrosion is still unclear.

The leached 14C from irradiated Zircaloy-2 under a pH of 12.5 was specified as gas and liquid phases. The gaseous 14C fraction decreases with time, instead an increasing release fraction of 14C in liquid phase with time was over 90% after 2 years. The inorganic/organic ratios in the liquid were around 1/3 and seemed to be not depending on time.

The instant release fraction (IRF) for hulls was also discussed through the experiment with irradiated Zircaloy having an oxide layer. The inventory measurement found that the abundance of 14C in the oxide was only 7.5%, which is less than 20% estimated in the safety case. Further, the leached 14C was found to be less than 0.01% of the total 14C activity after 6.5 years of immersion. These understandings should be reflected in the safety case that a lower IRF is justified or a negligible IRF is potentially suggested.

List of Contents

1 Contribution of KIT to WP3

1.1 *Introduction*

In assessments of the long-term safety of a repository for nuclear waste, ^{14}C is one of the key radionuclides with respect to estimated doses arising from the release in a canister failure scenario due to its long half-life and assumed mobility. However, ^{14}C is a difficult radionuclide to measure (soft β^--emitter and no γ-rays). Therefore, an elaborate and robust extraction and analysis technique is required. Details about the dissolution experiments and the ^{14}C extraction set-up can be found elsewhere [HERM *et al.*, 2015; HERM, 2015].

Only a few studies are available dealing with radiocarbon quantification in irradiated Zircaloy [GRAS, 2014; HERM, 2015]. Also the number of studies dealing with speciation of ^{14}C after release from irradiated Zircaloy is very limited [GRAS, 2014; HERM, 2015].

In this study, the amount and chemical form of ^{14}C, as well as the inventories of ^{55}Fe and ^{125}Sb, are determined in Zircaloy-4 cladding from an irradiated UO_2 fuel rod segment. Further details about the fuel rod segment and its power history are provided elsewhere [METZ *et al.*, 2014; HERM *et al.*, 2015; HERM, 2015].

Experimentally measured radionuclide contents are compared to the theoretically predicted inventory of the studied cladding obtained by means of MCNP/CINDER and SCALE/TRITON/ORIGEN-S calculations.

1.2 *Thermodynamic modelling of ^{14}C in Zircaloy*

After formation of ^{14}C in Zircaloy, the highly excited and charged carbon ion competes with available reactants and possibly forms carbides in reactions with metals. In corrosion layers of the cladding, oxygen is available which, in addition, possibly interacts with the formed ^{14}C. Thermodynamic properties of phases potentially containing ^{14}C in the Zircaloy cladding is described in the following.

In Zircaloy cladding the predominant mechanism leading to the formation of ^{14}C is due to reactions involving ^{14}N impurities present in the Zr-alloy. In the coolant/oxide layers, the oxygen isotope ^{17}O also contributes to the generation of ^{14}C. The principal formation reactions are: $^{14}N(n,p)^{14}C$, and $^{17}O(n,\alpha)^{14}C$. The yield of ^{14}C formed by these reactions depends on the amount of precursor elements, the neutron flux, the neutron energy, and thus from the local position in the nuclear reactor.

In Zircaloy, the excited ^{14}C, after formation, is surrounded by other metal atoms (Zr >> Sn > Fe, Cr, Ni > other metallic impurities present in Zircaloy). A possible reaction is:

$^{14}C + nMe \rightarrow Me_n{}^{14}C$ (where Me denotes other metal atoms).

Such compounds are called carbides. Assuming that nitrogen is homogeneously distributed in the Zircaloy matrix with an initial concentration of about 50 ppm, each ^{14}C is surrounded by about 3500 other metal atoms. These Me–C compounds are dispersed in the metal matrix and cannot form carbide crystals. Further, it is assumed that the formation of Me–C compounds consisting of several C atoms is unlikely.

1.2.1 Carbides

A carbide is a compound composed of carbon and a less electronegative element. Carbides can be generally classified by their chemical bonding type as follows:

- Salt-like carbides are composed of highly electropositive elements such as alkali metals, alkaline earth metals, and some group 3 metals (e.g. Al). These carbides feature isolated carbon centres. In contact with water, these carbides decompose forming methane (in the case of e.g. Al_4C_3) or acetylene (in the case of e.g. CaC_2).
- Covalent compounds, such as boron or silicon carbides.
- Interstitial compounds of the group 4, 5, and 6 transition metals (e.g. ZrC, WC, etc.). These carbides have metallic properties and they are refractory.
- Transition metal carbides showing multiple stoichiometries e.g. Fe_3C, Fe_7C_3, and Fe_2C.

Hardfacing alloys such as drill bits achieve their properties by deposit welding. The amount (volume) of the carbides formed and their structure, composition and degree of homogeneity determine the nature of the strengthening of the weld metal and thus its service characteristics. For this reason several data collections and reviews of thermodynamic data have been published [WICKS AND BLOCK, 1961; SHATYNSKI, 1979; IWAI *et al.*, 1986; FARKAS *et al.*, 1996; MAZUROVSKY *et al.*, 2004]. Carbides of the most abundant elements such as Al, Ca, Fe, Cr, Ni, Mo, Zr and Nb are listed in Table 1 with the corresponding standard free energy of formation $\Delta G_f°$ and/or functions for calculating the free energy of formation at various temperatures ΔG_f. ΔG_f^0 values for uranium and thorium carbides are also listed. According to Table 1, zirconium or niobium carbides (ZrC or NbC) may be formed in the cladding of the fuel rods. In industry, ZrC is used as a refractory metal in sub-stoichiometry. At carbon contents higher than approximately $ZrC_{0.98}$ the material contains free carbon. Stability range of ZrC covers carbon to metal ratios ranging from 0.65 to 0.98. It has a cubic crystal structure and is highly corrosion resistant. In addition, the formation of carbides with minor alloy components or trace impurities is assumed.

1.2.2 Oxides

Whereas in the metallic parts oxygen is not present, oxygen exits in the corrosion layers at the surfaces of the metals. Within these oxide layers, ^{14}C might be present in different forms:

- Sorbed species originating from the formation of ^{14}C in the coolant of the reactor.
- ^{14}C carbide or oxide species directly formed in these oxide layers.

Table 1: Free energy of formation for some relevant carbides of elements present in cladding materials and steel [WICKS AND BLOCK, 1961; SHATYNSKI, 1979].

Element	Compound	Free Energy of Formation [cal/mol]	T [K]
Ca	$2Ca + C \rightarrow Ca_2C$	$\Delta G_f = -16200$	298 [WICKS AND BLOCK, 1961]
Al	$4Al + 3C \rightarrow Al_4C_3$	$\Delta G_f = -36{,}150 + 8.02\times T\times \ln T - 8.35\times10^{-3}\times T^2 - 3.15\times10^{5}\times T^{-1} - 46.2\times T$	298 – 600 [WICKS AND BLOCK, 1961]
Fe	$3Fe + C \rightarrow Fe_3C$	$\Delta G_f = +4530 - 5.43T\times\ln T + 1.16\times10^{-3}T^2 - 0.40\times10^{5}T^{-1} + 31.98T$	298 – 463
		$\Delta G_f = +3850 - 11.41T\times\ln T + 9.66\times10^{-3}T^2 - 0.40\times10^{5}T^{-1} + 66.2T$	463 – 1033
		$\Delta G_f = +13130 + 9.68\times\ln T - 0.99\times10^{-3}T^2 - 1.05\times10^{5}T^{-1} - 78.14T$	1033 – 1179
		$\Delta G_f = -1000 - 7.0T\times\ln T + 3.5\times10^{-3}T^2 - 1.05\times10^{5}T^{-1} + 46.45T$	1179 – 1500
Cr	$\frac{7}{23} Cr_{23}C_6$	$\Delta G_f = -29985 - 7.41\times T$	1100 – 1720
Nb	$Nb + C \rightarrow NbC$	$\Delta G_f = -31100 + 0.4\times T$	1180 – 1370
	$2Nb + C \rightarrow Nb_2C$	$\Delta G_f = -46000 + 1.00\times T$	1180 – 1370
Mo	$2Mo + C \rightarrow Mo_2C$	$\Delta G_f = -12030 - 1.44\times T$	600 – 900
		$\Delta G_f = -11710 - 1.83\times T$	1200 – 1340
Ni	$3Ni + C \rightarrow Ni_3C$	$\Delta G_f = +8110 - 1.70\times T$	298 – 1000
Zr	$Zr + C \rightarrow ZrC$	$\Delta G_f = -44100 + 2.2\times T$	298 – 2220
Th	ThC_2	$\Delta G_f = -50000$	298 [WICKS AND BLOCK, 1961]
U	UC	$\Delta G_f = -43600$	298 [WICKS AND BLOCK, 1961]
	U_2C_3	$\Delta G_f = -78400$	298 [WICKS AND BLOCK, 1961]
	UC_2	$\Delta G_f = -37500$	298 [WICKS AND BLOCK, 1961]

In order to estimate the formation of oxide-carbon species such as ^{14}CO or $^{14}CO_2$, again the (standard) free energy of formation can be used. ΔG_f of the oxides depend on the temperature. Therefore, in some cases, oxidation is possible only in a specific temperature range. Thermodynamic calculations over a wide range of temperatures are generally performed by algebraic equations, representing the characteristic properties of the substances under consideration. The following equations for temperature extrapolations of the free energy of formation ΔG_f as well as the fitting parameters were taken from [GLASSNER, 1957]. For the reaction: $Me + nX_2 \rightarrow MeX_{2n}$, the free energy of formation is calculated by:

$$\Delta G_f(T) - \Delta H_{f,298} = -(2.303\Delta a)T \cdot \log T - 1/2(\Delta b \cdot 10^{-3})T^2 - 1/6(\Delta c \cdot 10^{-6})T^3 - (1/2(\Delta d \cdot 10^5))/T - T\Delta(B - a) - \Delta A$$

with $\Delta h = h(MeX_{2n}) - h(Me) - n \cdot h(X_2)$

Where $\Delta H_{f,298}$ is the enthalpy of formation at 298 K, $\Delta G_f(T)$ is the free energy of formation at given temperature *T*, and h incorporates the fit data a, b, c, d, (B-a) and A [GLASSNER, 1957].

The addition of carbon or CO(g) is used in metallurgy/industry e.g. to prevent alloy metals from oxidation.

- Nickel will undergo oxidation to nickel oxide (NiO) in an atmosphere with an oxygen potential greater than −251 kJ/mol at 1000°C, or −339 kJ/mol at 500°C, respectively.
- Chromium has a greater affinity for oxygen than nickel. It would require an oxygen potential of less than −544 kJ/mol at 1000°C to prevent oxidation.

Thus an atmosphere which is just adequate to prevent nickel from being oxidised would not protect chromium from oxidation. In many cases, the chemical stability of compounds decreases with increasing temperature (less negative ΔG_f). To estimate which oxidation reactions are favoured at different conditions, the oxygen potentials or ΔG_f values of some elements, water and the carbon species CO and CO_2 have been calculated as a function of

temperature and plotted as an Ellingham diagram (see Figure 1) using the data of [GLASSNER, 1957]. The stability of a metal oxide increases; the lower the line of the metal in the diagram is (i.e. more negative ΔG_f). A metal (e.g. Al) whose free energy of formation ΔG_f is lower than that of an oxide (e.g. Fe_2O_3) at a given temperature will reduce the oxide (e.g. to metallic Fe) and is oxidized itself (e.g. to Al_2O_3). Furthermore, the free energy of formation of CO_2 is almost temperature independent, while the stability of CO increases with temperature (Boudouard reaction).

Most elements of interest, such as Fe, Mn or Mo, have significantly lower ΔG_f values for forming oxides than the oxidation reactions of carbon. The only element which may compete for oxygen with carbon in the typical range of coolant temperatures is Ni (see Figure 1). The other elements under consideration such as Zr have significantly lower ΔG_f values ($\Delta G_f(ZrO_2) = -519$ kJ/mol oxygen). Also for water, the $\Delta G_f(H_2O) = -239$ kJ/mol oxygen at 300 K and exceeds the ($\Delta G_f(CO_2)$ only at temperatures above 900 K. The data shown in Figure 1 are also shown in Table 2.

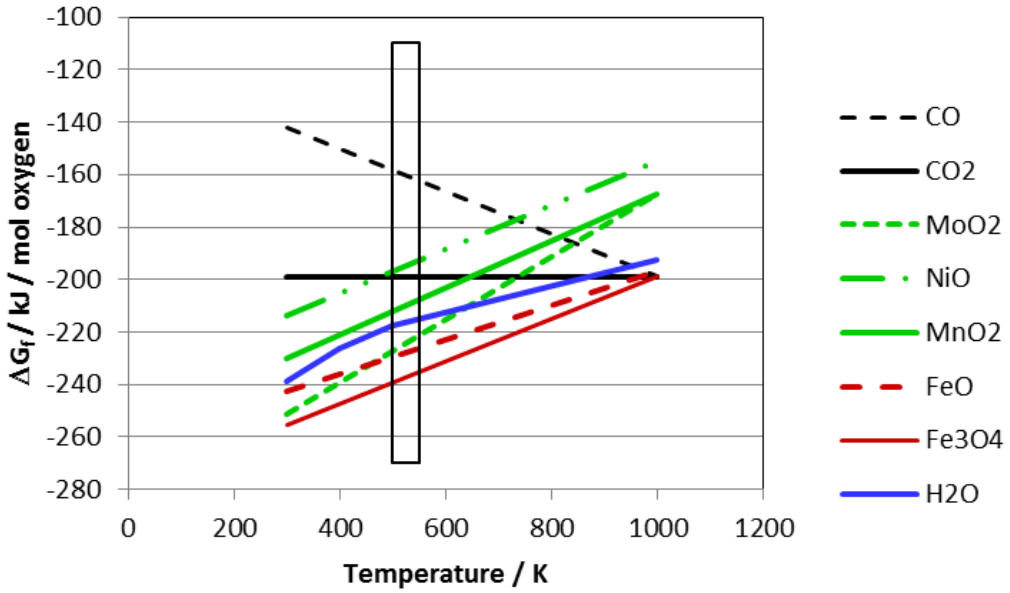

Figure 1: Free energy of formation for carbon oxides, Fe, Mo, Mn, and Ni oxides. The box indicates approximately the surface temperature of the cladding during reactor operation.

Table 2: Free energy of formation for some relevant elements of the surface layers of Zircaloy.

	Free energy of formation [kJ /(mol oxygen)]			
Temperature	**300 K**	**400 K**	**500 K**	**1000 K**
CO	-142			-199
CO_2	-199			-199
NiO	-214			-155
MnO_2	-230			-167
H_2O	-239	-226	-218	-193
FeO	-243			-197
MoO_2	-251			-167
Fe_3O_4	-255			-199
CrO_2	-272	-251		
Cr_2O_3	-348			-289
Nb_2O_5	-356			-297
MnO	-364			-314
NbO	-377			-327
SiO_2	-414			-348
ZrO_2	-519			-452
Al_2O_3	-523			-456

1.3 *Results and discussion*

1.3.1 Discussion on thermodynamic modelling of ^{14}C in Zircaloy

The results of the thermodynamic considerations for ^{14}C in Zircaloy are compared to [HICKS *et al.*, 2003] and [BUSH *et al.*, 1984]. Bush et al. investigated samples obtained from the Sizewell B PWR in UK. The authors showed amounts of ^{14}C typically produced in fuel, water coolant (assuming zero ppm nitrogen), Zircaloy cladding, stainless steel, and nickel alloy components of this PWR reactor. The amount of ^{14}C formed by the ^{17}O reaction in the water coolant/moderator is about 0.1–0.2 TBq/GW(e)yr. Bush et al. further discussed the fate of the ^{14}C in the different reactor materials and concluded that ^{14}C in the coolant is released in gaseous or dissolved forms from the reactor. Off-gases released from PWRs contain ^{14}C mostly in the form of methane and other hydrocarbons.

The results reported by Bush et al. are in agreement with the thermodynamic considerations performed in this study. ^{14}C-bearing carbides are formed in metals from neutron capture

reactions involving ^{14}N. A list of possible interstitial metallic-like carbides is given in Table 1. The interstitial carbides (group 4, 5, and 6 transition metals) have metallic properties, and react very slowly with water. The carbides of the transition metals are more reactive than the interstitial carbides and multiple stoichiometries (e.g. Fe_3C, Fe_7C_3, Fe_2C) can be found with Fe_3C also known to be present in steels [DURAND-CHARRE, 2004]. Especially the carbides of Fe, Cr, Ni, Mn, and Co are decomposed by dilute acids and also water, forming mixtures of hydrogen and hydrocarbons.

Different behaviour is seen for the salt-like carbides, which are formed with light elements such as calcium or aluminium, etc. Aluminium carbide Al_4C_3 or magnesium carbide Mg_2C react easily with water forming methane. Calcium carbide reacts with water forming acetylene. Impurities of these elements might be present in the coolant causing the release of gaseous hydrocarbon.

According to the thermodynamic data there is almost no driving force to form CO or CO_2 compounds after the formation of a ^{14}C atom. At the temperature range between 500 and 550 K of the coolant, only NiO could release oxygen to form CO_2. However below 500 K, this reaction is not possible. The same is true for water, which shows a much higher thermodynamic stability (lower ΔG_f) with respect to oxygen.

1.3.2 Inventory of ^{14}C in irradiated Zircaloy-4 cladding

The inventory of ^{14}C and other radionuclides present in irradiated Zircaloy-4 was determined independently in six specimens using acid digestion in a flask or an autoclave [HERM *et al.*, 2015].

The results of the inventory analysis in each of the six subsamples are shown in Table 3. Within the analytical uncertainty of the method, a good reproducibility of the experimentally-determined ^{14}C, ^{55}Fe, and ^{125}Sb activities is seen.

Table 3: Results obtained from LSC and γ-measurements from six Zircaloy-4 cladding specimens.

sample no.	**total ^{14}C** [Bq/g Zry-4]	**^{55}Fe** [Bq/g Zry-4]	**^{125}Sb** [Bq/g Zry-4]
#1	3.9 (±0.4)×10^4	1.3 (±0.1)×10^5	2.6 (±0.1)×10^5
#2	4.2 (±0.4)×10^4	ND	2.4 (±0.1)×10^5
#3	3.4 (±0.3)×10^4	ND	2.5 (±0.1)×10^5
#4	3.2 (±0.3)×10^4	ND	2.3 (±0.1)×10^5
#5	ND	1.7 (±0.2)×10^5	2.5 (±0.1)×10^5
#6	3.8 (±0.4)×10^4	ND	2.2 (±0.1)×10^5

ND: not determined

Mean values of the experimentally-determined radionuclide contents are shown in Table 4 and are compared to inventory calculations performed within this study. The activation of the fuel rod segment was calculated using two independent approaches: (i) The neutron flux of the subassembly was simulated using the Monte Carlo N-particle code (MCNP) and finally the CINDER program calculated the activation of the material [WILSON *et al.*, 2008; PELOWITZ, 2011]. (ii) The SCALE/TRITON package was used to develop cladding macro-cross-section libraries, which were used in the ORIGEN-S program to calculate the radioactive inventory of the cladding [GAULD *et al.*, 2009; ORNL, 2011].

Within the analytical uncertainty, the experimentally-determined contents of ^{14}C, ^{55}Fe, and ^{125}Sb are in good agreement with the calculated values. The experimental ^{14}C inventory agrees with the calculated values by a factor of about one . The two independent theoretical approaches also agree with each other.

Table 4: Mean values of the experimentally determined inventories of ^{14}C, ^{55}Fe, and ^{125}Sb in comparison with results from the activation calculations performed in the present study.

	total ^{14}C [Bq/g Zry-4]	**^{55}Fe** [Bq/g Zry-4]	**^{125}Sb** [Bq/g Zry-4]
experimentally determined inventory	3.7 (± 0.4)×10^4	1.5 (± 0.1)×10^5	2.4 (± 0.1)×10^5
calculated inventory (MCNP/CINDER)	3.5 (± 0.4)×10^4	1.3 (± 0.1)×10^5	2.6 (± 0.1)×10^5
calculated inventory (SCALE/TRITON/ORIGEN-S)	3.6 (± 0.4)×10^4		

1.3.3 Chemical form of ^{14}C after release from the cladding

Dissolution experiments performed in a glass reactor provided insight into the partitioning between inorganic and organic ^{14}C-bearing compounds released from Zircaloy. In addition, dissolution experiments performed in an autoclave provided information about the distribution of the released inorganic/organic ^{14}C-bearing compounds into the aqueous and gaseous phase.

Figure 2 shows the partitioning of ^{14}C-bearing compounds in inorganic/organic fractions and their distribution into the aqueous and/or gaseous phase. About (88 ± 10)% of the ^{14}C inventory present in the studied Zircaloy-4 is released as gaseous organic ^{14}C-bearing compounds into the gas phase during acid digestion. On the contrary, about (11 ± 10)% remains as dissolved organic ^{14}C-bearing compounds in the acidic digestion liquor. A very low content of inorganic ^{14}C-bearing compounds (< 1%) is found in all experiments, both in the gaseous and aqueous phases. The ratio between inorganic and organic ^{14}C-bearing compounds in the aqueous phase (1:390 ± 39) and gaseous phase (1:430 ± 43) is virtually the same, within the analytical uncertainty.

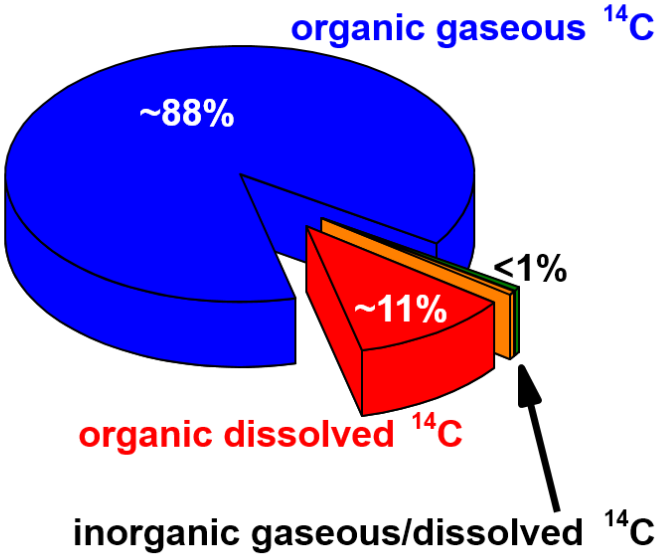

Figure 2: Partitioning of ^{14}C-bearing compounds in inorganic/organic fractions and their distribution into the aqueous and/or gaseous phase.

1.4 *Summary and outlook*

Using the ^{14}C separation and analysis techniques developed in this work for gaseous and aqueous samples derived from acid digestion of irradiated Zircaloy-4 specimens, it was possible to quantify the ^{14}C content in these samples. The partitioning of ^{14}C between inorganic and organic ^{14}C-bearing compounds and their distribution between solution and gas phase was also investigated. In addition to ^{14}C, the contents of ^{55}Fe and ^{125}Sb in irradiated Zircaloy-4 were analysed and also compared to MCNP/CINDER and SCALE/TRITON/ORIGEN-S calculations.

Taking into account the related uncertainties (e.g. limited availability of data for the calculations), the experimentally-determined activities of the activation products in the irradiated Zircaloy-4 are indistinguishable from the calculation-derived values; this builds confidence in the results and understanding gained.

The combination of glass reactor and autoclave experiments allowed knowledge to be gained not only about the partitioning of ^{14}C between inorganic and organic ^{14}C-bearing compounds, but also about the distribution of these compounds in solution and gas phase.

Leaching experiments under alkaline conditions (0.01 M NaOH solution) are to be undertaken, to complement work reported herein. However, these experiments will be conducted outside of the CAST project.

2 Contribution of RWMC to WP3

2.1 *Corrosion rate of unirradiated and irradiated Zircaloys*

Unirradiated Zr, Zircaloy-4 and Zircaloy-2 were obtained from CEZUS Co., Ltd. The samples were polished with 0.02 mm alumina powder. The initial hydrogen content was measured and found to be lower than 10 ppm. The samples were immersed in appropriate solutions. The corrosion rate can be obtained from the rate and cumulative total amount of generated hydrogen (gas and absorbed), based on the following reaction:

$$Zr + 2H_2O \rightarrow ZrO_2 + 2H_2 \qquad (1)$$

Irradiated Zircaloy-2 hulls (BWR claddings), without an oxide film, were immersed in a dilute NaOH solution at pH 12.5 and under a nitrogen atmosphere at room temperature (around 293 K).

^{14}C in both gas and aqueous phases was measured by liquid scintillation counting (LSC). Assuming that the activated ^{14}C is distributed homogeneously in the cladding and a congruent ^{14}C release with the CR, the equivalent corrosion rate, R_{eq}, can be obtained from:

$$R_{eq} = \frac{aL}{2At} \qquad (2)$$

where, a is the leached amount of ^{14}C (Bq), A is the inventory in the cladding (Bq), L is the thickness of the cladding (μm), and t is the test time (years).

Figure 3 shows the results of the corrosion rate for unirradiated Zircaloys and the equivalent corrosion rate for irradiated Zircaloy. The corrosion rate decreases with time and increases as the temperature increases. Through these corrosion tests, the hydrogen pickup ratios showed high percentages at around 95% for 303 K, 90% at 323 K, and 85% for 353 K, respectively. The equivalent corrosion rate of irradiated hulls determined by ^{14}C release is less than that of unirradiated Zircaloy determined by H_2 release; in part this is attributed to the effect of temperature. However, the congruence of ^{14}C leaching with corrosion has not been confirmed yet and is a future challenge.

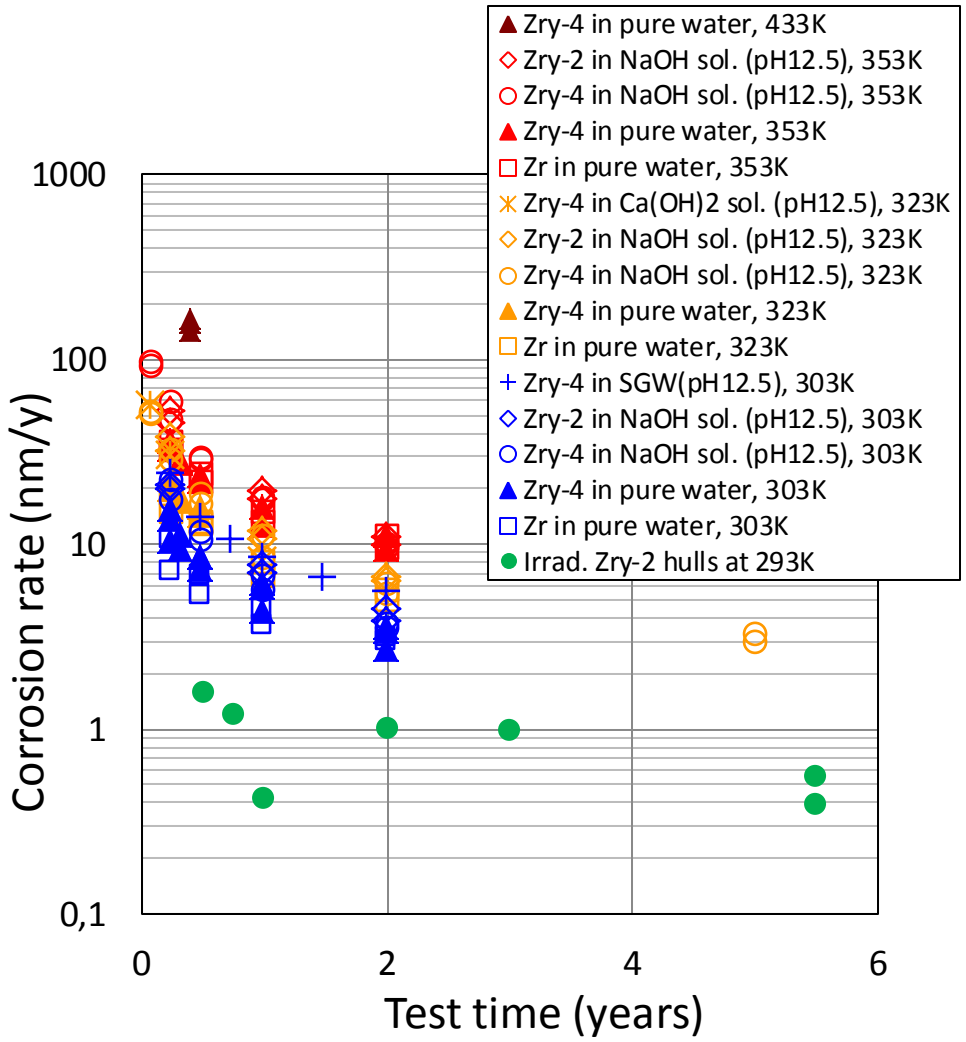

Figure 3: Corrosion rate for unirradiated Zircaloys obtained by hydrogen measurement under different conditions and for irradiated Zircaloy-2 hull (BWR cladding without oxide) obtained from leached ^{14}C in a NaOH solution (pH 12.5) at 293K.

2.2 *Chemical form of released ^{14}C from irradiated Zircaloy*

As described in the section above, the leaching test using irradiated Zircaloy-2 hulls was performed and the distribution of ^{14}C in liquid and gas phases are shown in Figure 4. The results for the samples without the oxide layer show a release of ^{14}C to gas and liquid phases, with a significant fraction released as gas (53-55%) during the first year. As the experiments continue, however, the fraction of ^{14}C released as gas decreases relative to the

release to liquid phase, with a maximum release fraction of gas up to 5-6% after one year to 5.5 years. In the case of samples with external oxide layer, the release fraction of ^{14}C in the gas phase is 16%. In the liquid phase, ^{14}C is dissolved as inorganic and organic compounds, with an increasing fraction of the organic form with time: the associated ratio of inorganic/organic ^{14}C evolves from 2/3 to 1/3.

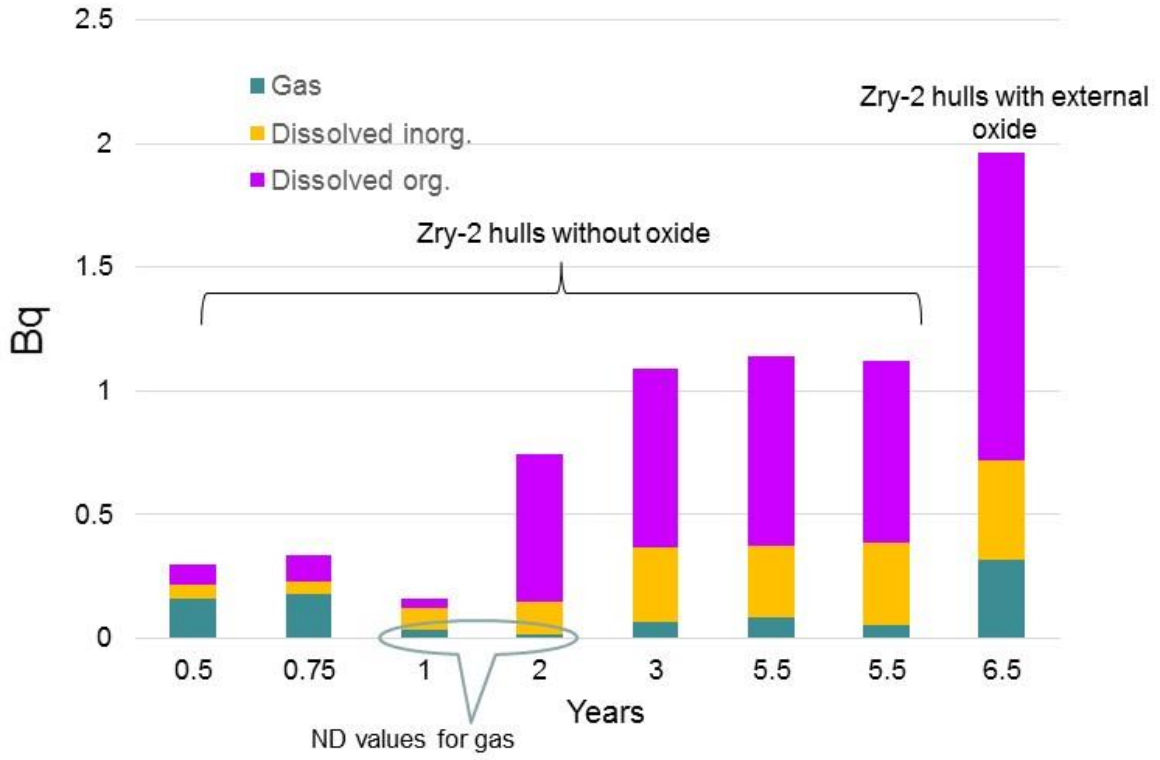

Figure 4: Leached ^{14}C and speciation in gas and liquid phases from irradiated BWR cladding.

2.3 *Instant release fraction (IRF) for Zircaloy hulls*

The radionuclides in hull oxide are regarded as a source of an instant release fraction (IRF) in the preliminary Japanese safety case, in which 20% of ^{14}C in cladding was assumed as an IRF and the remaining 80% was assumed to be in the form of a corrosion-related congruent release from the base Zircaloy metal [FPEC/JAEA, 2007]. In order to investigate the IRF,

the ^{14}C inventory in oxide has been measured using irradiated cladding with a 25.3 μm thick external oxide film (Zircaloy-2, average rod burnup of 41.6 GWd/t_U) at first. Then, a static leaching test was carried out for 6.5 years using cladding tube whose internal oxide was removed. The major leaching source (oxide or base metal) is discussed in the following section.

The prepared samples for ^{14}C measurement are shown in Figure 5 and the results are summarized in Table 5. The specific activity (Bq/g) between oxide and base Zircaloy differs by a factor of 2.8. This is maybe due to the additional activation reaction of $^{17}O(n,\alpha)^{14}C$ in the oxide layer. However, the abundance of ^{14}C in the oxide and the base Zircaloy, which is obtained from cladding geometry, can be estimated as 7.5% and 92.5%, respectively. This ^{14}C distribution corresponds roughly to the ^{14}C inventory in waste claddings estimated by the ORIGEN calculation in previous work [SAKURAGI *et al.*, 2013], in which the respective percentages of 3.5% and 96.5% were suggested for the BWR cladding. It can therefore be concluded from the results of both the measurements in this study and previous calculations that the assumption of 20% IRF as has been used in some safety case studies [FPEC/JAEA, 2007] is conservative; a lower IRF is justified in the work reported herein.

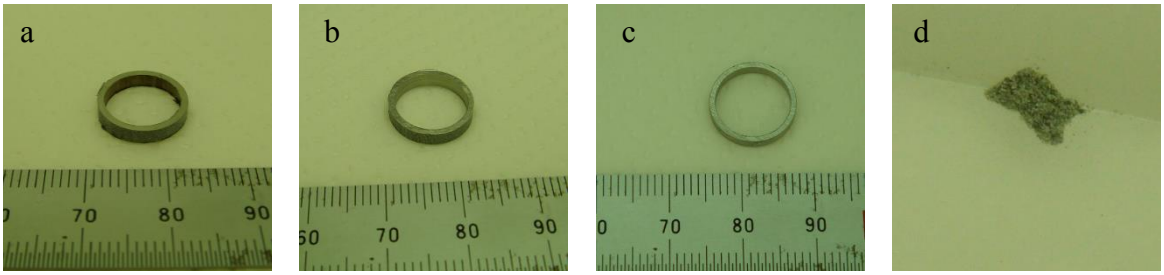

Figure 5: Photographs showing irradiated Zr claddings: (a) with internal and external oxide layers in place, (b) with internal oxide removed, (c) with internal and external oxide removed, (d) (external) oxide fragment removed from the cladding [SAKURAGI *et al.*, 2016].

Table 5: Specific activity of ^{14}C for irradiated Zircaloy and oxide [SAKURAGI *et al.*, 2016].

Thickness (μm)		Specific activity (Bq/g)			
Base metal	Oxide layer	(a) Cladding with internal and external oxide	(b) Cladding with external oxide	(c) Cladding base metal	(d) External oxide*
704.7	25.3	1.54×10^4	1.53×10^4	1.49×10^4	4.25×10^4
		1.49×10^4		1.50×10^4	3.83×10^4
		1.43×10^4		1.47×10^4	

* Units of grams in the oxide are converted to grams of zirconium, not grams of ZrO_2.

The results of leaching tests are shown in Figure 6, together with the results for Zircaloy hulls with and without oxide. The leaching ratio, which represents the leached amount (gaseous + dissolved) divided by the initial inventory, is very low (0.0038%) for the hull with external oxide after 6.5 years in NaOH solution. The previous short-term leaching tests for PWR hulls with inner and external oxide also showed small leaching ratios [YAMAGUCHI *et al.*, 1999]. Based on the assumption that the radionuclide release from the Zircaloy matrix is regarded as a corrosion-related congruent release, the released fraction of ^{14}C from the hull with external oxide was estimated as 96.7% from external oxide and 3.3% from base Zircaloy metal [SAKURAGI *et al.*, 2016]. This leads to the conclusion that the main source of ^{14}C release is from the oxide. However, regarding the ^{14}C in oxide as an IRF would be overly conservative, because the total released ^{14}C from the hull with oxide after 6.5 years of immersion is 0.0038% of the total C-14 activity in the hull. Both the low amount of ^{14}C in oxide and the low leaching rate indicate that the ^{14}C in oxide does not have

a major impact on the instant release fraction; this understanding should be reflected in the safety case. If not instant release, other mechanisms need to be taken into account to explain ^{14}C release from the oxide.

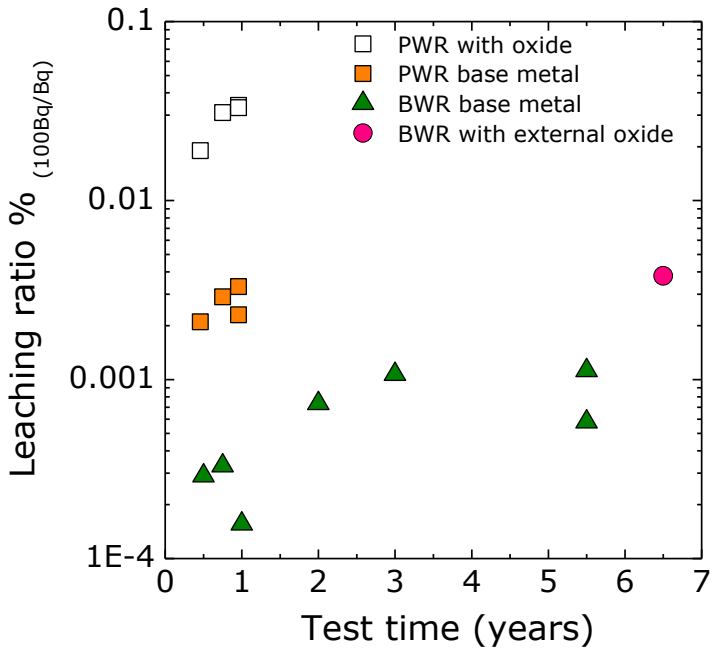

Figure 6: Leached ^{14}C from irradiated Zr claddings: PWR with oxide (white square), PWR without oxide (orange square) [YAMAGUCHI *et al.*, 1999], BWR without oxide (green triangle), and BWR with external oxide (pink circle) [SAKURAGI *et al.*, 2016].

3 General conclusions

Although the digestion experiments of KIT were performed under acidic conditions, clearly outside of repository-relevant conditions, little impact on the chemical form of ^{14}C released from irradiated Zircaloy under repository relevant conditions is expected. The majority of ^{14}C is found as dissolved/gaseous hydrocarbons and almost no dependency on the pH is expected for organic compounds [BLEIER *et al.*, 1988]. Of course the experiments allowed neither to evaluate release rates of ^{14}C nor to assess the stability of the released compounds. However, strongly reducing conditions potentially developing in a deep underground repository for nuclear waste favour the formation of reduced/organic ^{14}C-bearing compounds. The results obtained in this study could therefore have implications on safety analyses of deep geological repositories for nuclear waste, wherein ^{14}C is typically and conservatively assumed to be highly mobile in the aqueous and gaseous phase either as dissolved or gaseous hydrocarbons i.e. such ^{14}C-bearing compounds are possibly transported into the biosphere, where ^{14}C is metabolized by any kind of organism.

RWMC obtained the corrosion rate for nonirradiated by the hydrogen measurement. The corrosion rates decreased with time and increased as the temperature increased, but the influence of pH and other chemical components of the solution on the rate was not significant. The equivalent corrosion rate of irradiated Zircaloy-2 obtained from leached 14C assumed congruence with corrosion was less than that of unirradiated Zircaloy. Since this can not be sufficiently explained with only the difference of the test condition (temperature), the congruence of 14C leaching with corrosion has not been confirmed yet and is a future challenge.

The leached 14C from irradiated Zircaloy-2 under a pH of 12.5 was specified as gas and liquid phases. The gaseous 14C fraction decreases with time, instead an increasing release fraction of 14C in liquid phase with time was over 90% after 2 years. The inorganic/organic ratios in the liquid were around 1/3 and seemed to be not depending on time. The corroded condition such as pH could affect the formation of carbon species, especially acidic conditions are likely to form hydrocarbons as gaseous organic species seen in KIT's work in this report. Reaction time during corrosion/dissolution process is also a key factor

affecting the formation of carbon-bearing compound: the rapid dissolution is likely to keep the carbon species as it was presented in Zircaloy matrix, but the oxidation forming some organic acids seems to be a required reasonable reaction time.

The instant release fraction (IRF) for hulls was discussed with the experimentally obtained 14C inventory in the oxide and the leached 14C from irradiated cladding having an external oxide layer. The main results were the abundance of 14C in the oxide with an estimated IRF of 7.5%, and the leached 14C was 0.0038% of the total 14C activity after 6.5 years of immersion. This understanding should be reflected in the safety case that a lower IRF is justified or a negligible IRF is potentially suggested.

Acknowledgements

This research is a part of the "Research and development of processing and disposal technique for TRU waste" program funded by Agency for Natural Resources and Energy, Ministry of Economy, Trade and Industry of Japan.

References

Federation of Electric Power Companies (FEPC) and Japan Atomic Energy Agency (JAEA), Second progress report on research and development for TRU waste disposal in Japan, 2007.

BLEIER, A., BEUERLE, M., ELLINGER, M., AND BOHLEN, D. 1988. Untersuchungen zum chemischen Status von C14 nach Auslaugung mit einer Salzlösung aus Hüllmaterial bestrahlter DWR- und SWR-Brennelemente. *Siemens, KWU*, U9 414/88/001.

BUSH, R. P., SMITH, G. M., AND WHITE, I. F. 1984. Carbon-14 waste management. EUR 8749 EN.

DURAND-CHARRE, M. 2004. *Microstructure of steels and cast irons* (Berlin Heidelberg: Springer-Verlag Berlin Heidelberg).

FARKAS, D. M., GROZA, J. R., AND MUKHEJEE, A. K. 1996. Thermodynamic analysis of carbide precipitates in a niobium-zirconium carbon alloy. *Scripta Materialia*, Vol. 34, 103-110.

GAULD, I. C., HERMANN, O. W., AND WESTFALL, R. M. 2009. ORIGEN scale system module to calculate fuel depletion, actinide transmutation, fission product buildup and decay, and associated radiation terms. *Oak Ridge National Laboratory*, ORNL/TM 2005/39, Version 6, Vol. II, Sect. F7.

GLASSNER, A. 1957. The thermochemical properties of the oxides, fluorides, and chlorides to 2500°K. *Argonne National Laboratory*, ANL-5750.

GRAS, J.-M. 2014. State of the art of ^{14}C in Zircaloy and Zr alloys - ^{14}C release from zirconium alloy hulls (D3.1). *CArbon-14 Source Term WP3 Deliverable D3.1*, CAST-D3.1.

HERM, M., GONZÁLEZ-ROBLES, E., BÖTTLE, M., MÜLLER, N., PAPAIOANNOU, D., WEGEN, D. H., DAGAN, R., KIENZLER, B., AND METZ, V. 2015. Description of Zircaloy-4 dissolution experiment in a shielded box (D3.8). *CArbon-14 Source Term – CAST*, Available from http://www.projectcast.eu/cms-file/get/iFileId/2493.

HERM, M. 2015. Study on the effect of speciation on radionuclide mobilization – C-14 speciation in irradiated Zircaloy-4 cladding and nitrate/chloride interaction with An(III)/Ln(III). Karlsruhe Institute of Technology (KIT). Available from http://dx.doi.org/10.5445/IR/1000051441.

HICKS, T. W., CRAWFORD, M. B., AND BENNET, D. G. 2003. Carbon-14 in radioactive wastes and mechanisms for its release from a repository as gas. 0142-1.

IWAI, T., TAKAHASHI, I., AND HANDA, M. 1986. Gibbs free energies of formation of molybdenum carbide and tungsten carbide from 1173 to 1573 K. *Metallurgical Transactions A*, Vol. 17, 2031-2034. In English.

MAZUROVSKY, V., ZINIGRAD, M., LEONTIEV, L., AND LISIN, V. 2004 CARBIDE FORMATION DURING CRYSTALLIZATION UPON WELDING. Ariel University, Israel.

METZ, V., GONZALEZ-ROBLES, E., AND KIENZLER, B. 2014. Characterization of UOX fuel segments irradiated in the Gösgen pressurized water reactor. *KIT Scientific Publishing*, KIT-SR 7676, http://dx.doi.org/10.5445/KSP/1000041743.

ORNL 2011. SCALE: a comprehensive modeling and simulation suite for nuclear safety analysis and design. *Oak Ridge National Laboratory*, ORNL/TM-2005-39, Version 6.

PELOWITZ, D. B. 2011. MCNPX Users Manual Version 2.7.0. LA-CP-11-00438.

SAKURAGI, T., TANABE, H., HIROSE, E., SAKASHITA, A., AND NISHIMURA, T. 2013. Estimation of Carbon 14 Inventory in Hull and End-Piece Wastes from Japanese Commercial Reprocessing Operation. *Proceedings of the ICEM2013. Brussels, Belgium*.

SAKURAGI, T., YAMASHITA, Y., AKAGI, M., AND TAKAHASHI, Y. 2016. Carbon 14 distribution in irradiated BWR fuel cladding and released carbon 14 after aqueous immersion of 6.5 years. *Procedia Chemistry,* Vol. 21, 341-348.

SHATYNSKI, S. R. 1979. The Thermochemistry of Transition Metal Carbides. *Oxidation of Metals,* Vol. 13, 105-118.

WICKS, C. E. AND BLOCK, F. E. 1961. Thermodynamic properties of 65 elements -Their oxides, halides,carbides, and nitrides. Bulletin 605. NP-13622.

WILSON, W. B., COWELL, S. T., ENGLAND, T. R., HAYES, A. C., AND MOLLER, P. 2008. A Manual for CINDER'90 Version 07.4 Codes and Data. LA-UR-07-8412.

YAMAGUCHI, T., TANUMA, S., YASUTOMI, I., NAKAYAMA, T., TANABE, H., KATSURAI, K., KAWAMURA, W., MAEDA, K., KITAO, H., AND SAIGUSA, M. 1999. A Study on Chemical Forms and Migration Behavior of Radionuclides in Hull Wastes. *Proceedings of the 7th International Conference on Environmental Remediation and Radioactive Waste Management - ICEM 1999. Nagoya, Japan.*